Downloaded from http://jgs.lyellcollection.org/ at Helmholtz-Zentrum fur Ozeanforschung Kiel on May 28, 2020

Accepted Manuscript

Journal of the Geological Society

The Paleogene Ophiolite Conundrum of the Iran-Iraq Border Region

Hadi Shafaii Moghadam, Qiu-Li Li, Robert J. Stern, Massimo Chiaradia, Orhan Karsli & Bahman Rahimzadeh

DOI: https://doi.org/10.1144/jgs2020-009

Received 14 January 2020
Revised 16 April 2020
Accepted 11 May 2020

© 2020 The Author(s). Published by The Geological Society of London. All rights reserved. For permissions: http://www.geolsoc.org.uk/permissions. Publishing disclaimer: www.geolsoc.org.uk/pub_ethics

Supplementary material at https://doi.org/10.6084/m9.figshare.c.4972994

When citing this article please include the DOI provided above.

Manuscript version: Accepted Manuscript
This is a PDF of an unedited manuscript that has been accepted for publication. The manuscript will undergo copyediting, typesetting and correction before it is published in its final form. Please note that during the production process errors may be discovered which could affect the content, and all legal disclaimers that apply to the journal pertain.

Although reasonable efforts have been made to obtain all necessary permissions from third parties to include their copyrighted content within this article, their full citation and copyright line may not be present in this Accepted Manuscript version. Before using any content from this article, please refer to the Version of Record once published for full citation and copyright details, as permissions may be required.

Downloaded from http://jgs.lyellcollection.org/ at Helmholtz-Zentrum fur Ozeanforschung Kiel on May 28, 2020

The Paleogene Ophiolite Conundrum of the Iran-Iraq Border Region

Hadi Shafaii Moghadam[1,2,3*], Qiu-Li Li[3], Robert J. Stern[4], Massimo Chiaradia[5], Orhan Karsli[6], Bahman Rahimzadeh[7]

[1]School of Earth Sciences, Damghan University, Damghan 36716-41167, Iran

[2]FB4-Dynamics of the Ocean Floor, GEOMAR, Helmholtz-Zentrum für Ozeanforschung Kiel, Wischhofstr. 1-3, 24148 Kiel, Germany

[3]State Key Laboratory of Lithospheric Evolution, Institute of Geology and Geophysics, Chinese Academy of Geosciences, Beijing 100029, China

[4]Geosciences Dept. University of Texas at Dallas, TX 75083-0688, USA

[5]Department of Earth Sciences, University of Genève, Genève, Switzerland

[6]Deptartment of Geological Engineering, RTE University, Rize TR-53000, Turkey

[7]Faculty of Earth Sciences, Shahid Beheshti University, Tehran, Iran

***Corresponding author:** Hadi Shafaii Moghadam, Tel: +49-17665306570, E-mail: hshafaei@geomar.de

Keywords: Neotethys, Ophiolite, Paleogene, Forearc Rift, Urumieh-Dokhtar Magmatic Belt, Iran

Abstract

New and compiled geochemical, isotopic, and geochronological data allow us to propose a new explanation for Paleogene oceanic magmatic rocks along the Iran-Iraq border. These rocks are represented by a thick pile (>1000m) of pillow lavas and pelagic sediments and underlying plutonic rocks. These are sometimes argued to represent a Paleogene ophiolite but there are no associated mantle rocks. Integrated zircon U-Pb ages, bulk rock major and trace element and radiogenic isotope data indicate that these rocks are more likely related to forearc rifting due to extreme extension during Late Paleogene time which also triggered high-flux magmatism in the Urumieh-Dokhtar Magmatic Belt and exhumation of core complexes in Iran. These observations are most consistent with formation of the Paleogene oceanic igneous rocks in a >220 km long forearc rift zone.

ACCEPTED MANUSCRIPT

Iran and Iraq contain many ophiolites of Mesozoic (mostly Late Cretaceous) age (Moghadam & Stern 2015). Late Cretaceous ophiolites are especially abundant along the Zagros suture zone of Iran and Iraq. Geochronological and geochemical data from Zagros ophiolites strongly support Neotethyan subduction initiation (SI) beneath SW Eurasia during earliest Late Cretaceous and maturation of the convergent margin in latest Cretaceous and Paleogene time (e.g., Golonka 2004; Moghadam & Stern 2011; Moghadam & Stern 2015; Nouri et al. 2016; Monsef et al. 2018). Subduction initiation was coincident with equivalent ophiolites in Oman and the eastern Mediterranean area (Cyprus, Turkey, Syria to Iraq) (Dilek et al. 2007; Dilek & Thy 2009; Moghadam & Stern 2011; van Hinsbergen et al.

Downloaded from http://jgs.lyellcollection.org/ at Helmholtz-Zentrum fur Ozeanforschung Kiel on May 28, 2020

2019). Late Cretaceous ophiolites are intruded and covered by younger, Cenozoic intrusions and volcano-sedimentary rocks. Abundant Cenozoic igneous rocks in Iran are readily distinguished because they tend to be felsic and eruptions were subaerial or in shallow water. However, along the Iran-Iraq border Cenozoic igneous rocks are often mafic and submarine and are easily confused with Late Cretaceous ophiolites (Figs. 1a-b). The presence of gabbros and overlying pillow lavas has led to these being described as a Paleogene ophiolite (e.g., Ao et al. 2016). Do Paleogene mafic-submarine mafic igneous rocks along the Iran-Iraq border really represent oceanic crust? Crucially, what is their significance in the framework of Neotethyan ophiolite and SW Eurasian tectonic evolution?

There are several interpretations for the genesis of these rocks. For example, (Saccani et al. 2014) described these rocks as Permian-Triassic passive margin-type ophiolite related to the Gondwana rifting and Neotethyan opening. Paleocene-Oligocene arc to back-arc basin models are also used to explain the occurrence of these rocks along the Zagros suture zone (Azizi et al. 2011a; Ali et al. 2013). A complex model involving Paleocene back-arc rifting and Eocene arc construction within the Paleocene back-arc basin along the Eurasian continental margin is also used to explain the occurrence of these rocks (Whitechurch et al. 2013). (Ao et al. 2016) argued that the Paleogene oceanic realm reflected an exhumed Eocene oceanic core complex, which triggered remelting of oceanic gabbros to make Paleogene granites. Another model considers slab breakoff- following Early Paleogene continental collision- and development of a slab window which facilitated partial melting of metasomatized lithospheric mantle to make Paleogene igneous rocks along the Iran-Anatolia margin (Dilek & Altunkaynak 2010). This controversy is usefully referred to as the Paleogene ophiolite conundrum.

In this paper, we report new data on Paleogene magmatic assemblages near Kermanshah-Kamyaran, Iran near the Iran-Iraq border region. We report new whole rock major and trace element and whole rock Sr-Nd-Pb isotope data along with zircon U-Pb ages and O-Hf isotopes and use these to better understand the age, geochemical signatures and source of these rocks. We further integrate our new data with published results to resolve the "Paleogene ophiolite conundrum" and identify for the first time an important Eocene oceanic rift zone that developed along the present border of Iran and Iraq with possible continuation into easternmost Turkey (Fig. 1b).

Late Cretaceous forearc ophiolites of the Iran-Iraq border region

Late Cretaceous SI-related Zagros ophiolites are present in the Kurdistan region of eastern Iraq and western Iran, around Kermanshah and Sahneh-Harsin (Fig. 1b). These ophiolites continue to the SE toward Neyriz and Haji-Abad ophiolites (Fig. 1A). Ophiolites in Kurdistan region are associated with thick Triassic-Cretaceous sequence of pelagic limestones (Avroman-Bisotun limestones), radiolarites (Qulqula-Kermanshah radiolarites) and OIB-, E-MORB-like lavas and minor felsic intrusive and extrusive rocks which are similar to Triassic (*ca* 230 Ma) alkaline magmatism of the Hawasina Nappes of Oman (Chauvet et al. 2011). These units are found near the Main Zagros Thrust (MZT; Figs. 1b-c) and are highly crushed. The along-strike continuation of these units to the SE is

ACCEPTED MANUSCRIPT

Downloaded from http://jgs.lyellcollection.org/ at Helmholtz-Zentrum fur Ozeanforschung Kiel on May 28, 2020

known as the Pichakun series in Neyriz, which consist of upper Triassic limestones, middle Jurassic oolitic limestones and lower-middle Cretaceous conglomeratic limestones. Minor OIB-like lavas accompany these sediments (Babaei et al. 2005).

These sequences are related to rifting of Gondwana and opening of Neo-Tethys. These units continue into Iraqi Kurdistan (Mawat to Hasanbag, Fig. 1b) where they are known as the Avroman limestones and Qulqula radiolarites.

The Late Cretaceous forearc ophiolite around Kermanshah include mantle peridotite, gabbro, minor plagiogranite, Nb-Ta depleted arc tholeiitic to calc-alkaline lava and Turonian-Maastrichtian pelagic limestone. Gabbroic dikes within the Kermanshah ophiolite mantle section are dated at *ca* 97 Ma and Kermanshah plagiogranites have zircon U-Pb ages of 94.6±2.7 to 99.5±0.2 Ma (Nouri et al. 2016). Further to the SE, in Neyriz and Haj-Abad, Late Cretaceous ophiolites includes depleted to highly impregnated harzburgites containing screens of residual dunite, chromitite, pyroxenitic sills/dikes, pegmatite gabbros and diabasic-basaltic-andesitic dikes. Sheeted dikes and pillow lavas construct the crustal sequence of these ophiolites. $^{40}Ar/^{39}Ar$ age data from crustal plagiogranites yield ages of 92.07 ± 1.69 and 93.19 ± 2.48 Ma (Babaie et al. 2006), whereas zircon U-Pb data show ages of 100.1 ± 2.3 to 93.4 ± 1.3 Ma (Monsef et al. 2018).

Zagros ophiolites show strong supra-subduction zone geochemical signatures, both for mantle and crustal rocks (Ghazi et al. 2010; Moghadam et al. 2010; Moghadam & Stern 2011; Monsef et al. 2018). The crustal sequence of Zagros ophiolites is represented by MORB-like lavas similar to fore-arc basalts (FAB), arc tholeiites and boninites, similar to present-day forearcs (Ishizuka et al. 2014), although Zagros igneous rocks have stronger Nb-Ta depletion, variable mantle sources and contributions of various subduction components during their genesis (Moghadam et al. 2012; Moghadam et al. 2013b; Moghadam et al. 2014). Magmatic rocks with boninitic compositions (Ti/V<10 and a depleted REE pattern) occur in the Haj-Abad (egg-shaped pillow lavas), Neyriz (sheeted dike complex) and Kermanshah (massive lava) (Moghadam & Stern 2011; Moghadam et al. 2013a). Zagros MORB-like rocks both pre-date and post-date boninites. The Zagros system, like other intra-oceanic forearcs, finally erupted calc-alkaline felsic lavas Zagros rocks with Ti/V>10 and high V/Sc.

Paleogene oceanic tracts of the Iran-Iraq border region

Paleogene volcano-sedimentary rocks are abundant for >220 km long on either side of the Iran-Iraq border, from SE of Kermanshah to Hasanbag (Fig. 1b). These rocks are called the Walash and Naopurdan volcano-sedimentary sequences in Iraq; we informally call them Kamyran series here. Paleogene rocks also occur as bimodal intrusive rocks (~41 Ma alkaline gabbros and A_2-type granites) in NW parts of Piranshahr (Mazhari et al. 2009) (Fig. 1b). The Walash-Naopurdan-Kamyran (WNK) volcano-sedimentary rocks- along with intrusive rocks from NW Iran- are the western extension of the Urumieh-Dokhtar Magmatic Belt (UDMB), which represents the Paleogene magmatic arc of Iran to the east (Fig. 1a). These sequences are intruded by Paleogene granitoids and gabbros. The Walash

ACCEPTED MANUSCRIPT

Downloaded from http://jgs.lyellcollection.org/ at Helmholtz-Zentrum fur Ozeanforschung Kiel on May 28, 2020

and Naopurdan sequences consist of pillow and massive basalts, andesites and pyroclastic rocks associated with sandstones, limestones and cherts. The thickness of the Walash-Naopurdan series varies up to > 3000 m. These rocks are mixed and fault-bounded with Late Cretaceous Iraqi ophiolites and even Permian-Triassic OIB-type lavas and limestones (Ali et al. 2013; Hassan et al. 2015). Recent $^{40}Ar/^{39}Ar$ radiometric dating on basaltic-andesitic feldspars and whole rocks near Hasanbag indicates ages of *ca* 43-24 Ma; 43.01±0.15 on Walash and 34.33±0.91to 24.10±4.8 Ma on Naopurdan rocks (Ali et al. 2013). In the Mawat area, ^{40}Ar-^{39}Ar geochronological data indicate that Walash andesites erupted at 43.1±0.3, 40.1±0.3 and 32.3±0.4 Ma (Aswad et al. 2014). Igneous rocks of the Walash and Naopurdan series have subduction-related characteristics, and include both arc tholeiites and calc-alkaline rocks (Aswad 1999; Numan 2001; Aswad et al. 2011; Aziz et al. 2011a; Aziz et al. 2011b; Ali et al. 2013). These geochemical characteristics are similar to those of Eocene arc-related volcano-sedimentary rocks from Kamyaran (Azizi et al. 2011b). The formation of the Walash and Naopurdan volcano-sedimentary series has been ascribed to an intra-oceanic convergent margin and development of an arc-back-arc setting during Paleocene-Oligocene (and even Miocene) time (Ali et al. 2013). Eocene volcano-sedimentary rocks are similarly present along the Bitlis-Zagros suture zone in SE Turkey, where their genesis is ascribed to Neotethys subduction, slab detachment, extension and melting of a sub-continental lithospheric mantle (Dilek et al. 2010).

The Paleogene intrusive rocks also occur around Kamyaran and are dominated at SE of Kermanshah, in Sahneh and Harsin. In around Kamyaran, these rocks intrude both Late Cretaceous ophiolitic rocks-especially serpentinites and harzburgites- and Paleogene volcanosediments and lavas (Figs. 1c-d). SE Kermanshah rocks includes gabbros, granitoids and pillow lavas with arc tholeiitic signature and high εNd(t) values (+3.7 to +9.8) (Nouri et al. 2017). Granites show a zircon U-Pb age of 35.7 ± 0.5 Ma (Ao et al. 2016). Granites and gabbros from Sahneh-Harsin intruded into Late Cretaceous harzburgites and Eocene volcanosediments (Whitechurch et al. 2013). (Azizi et al. 2011b) also described a series of calc-alkaline to arc tholeiitic pillow basalts (Fig. 2a) and gabbros SE of Kamyaran, with zircon U-Pb ages of 54.6 ± 0.3 Ma and 36.75 ± 0.51 to 36.63 ± 0.40 Ma respectively. Initial εNd of these rocks is high (+2.8 to +10), similar to those of intra-oceanic arcs (Azizi et al. 2011b). There is also an (basaltic-) andesitic to dacitic dike complex that is intruded by granitic lenses (Fig. 2b). Paleogene dikes intruded Late Cretaceous Kermanshah ophiolites and Paleogene lavas cover them. We sampled dikes as well as lavas for geochemical-isotopic analysis and granites-dacitic dikes for zircon U-Pb dating.

Paleogene oceanic sequences are also present NW of Kamyaran (E of Sarve Abad, Figs. 1b-c). This Paleogene sequence includes gabbros, diorites and granitic dikes at the lower parts with thickness of ~3-4 km (Figs. 2c-e). The lower gabbroic-dioritic sequence grades into a thick pile (>1000m) of pillow lavas (Figs. 2f-g). The abundance of granitic dikes increases toward the contact of the intrusive rocks with pillow lavas. Gabbros and granites show intrusive contacts with both Paleogene volcanosediments-sandstones and with thin slices of Late Cretaceous serpentinized

ACCEPTED MANUSCRIPT

Downloaded from http://jgs.lyellcollection.org/ at Helmholtz-Zentrum fur Ozeanforschung Kiel on May 28, 2020

harzburgites. To the WSW, this Paleogene sequence shows faulted contacts with Kermanshah radiolarites whereas in the ENE it has faulted contacts with Mesozoic rocks of the Sanandaj-Sirjan zone.

Analytical procedures

We used five analytical techniques including; 1- Cameca IMS-1280/HR SIMS and 2- LA-ICPMS to analyze zircons for U-Pb ages and O isotopes; 3- Multicollector-inductively coupled plasma-mass spectrometer (MC-LA-ICPMS) for analyzing Lu-Hf isotope composition of dated zircons; 4- X-ray florescence (XRF) and ICP-MS methods to analyze whole rock major and trace elements; and 5- Thermo Neptune PLUS Multi-Collector ICP-MS to analyze whole rock Sr, Nd and Pb isotopes. Detailed analytical procedure can be found in Appendix A.

Zircon U-Pb geochronology and O-Hf isotopes

We analysed four samples of Paleogene igneous rocks from near Kamyran. Gabbros (sample KN14-14, from the lower part of the section) and granitic dike (sample KN14-3 which intrudes gabbros) from NW of Kamyaran (E of Sarve Abad, Fig. 1c) have intercept ages of 39.7±0.5 Ma (Fig. 3b) and 39.5±0.3 Ma (Fig. 3a), respectively. Two samples of SE Kamyaran dacitic dikes and granites (crosscutting dikes) have concordia ages of 39.4±0.1 Ma (Fig. 3d) and 36.9±0.1 Ma (Fig. 3c), respectively. These are related magmatic pulses that generated a significant igneous crust in a very short time.

The εHf(t) values for NW Kamyaran granitic zircons range from +10.5 to +16.3, whereas gabbro zircons have overlapping and slightly higher εHf(t) values of +12.4 to +18.8. The $\delta^{18}O$ values vary from +5.3 to +7‰ for granitic dike zircons and to overlapping and slightly lower values from +4.9 to +5.7‰ for gabbro zircons. The εHf(t) values for SE Kamyaran rocks varies from -0.8 to -7.6, indicating an unradiogenic source for these magmas (Fig. 4b), perhaps reflecting involvement of Cadomian continental crust.

Whole rock major-trace elements and Sr-Nd-Pb isotopes

We analysed Paleogene gabbros, pillow lavas and granitic dikes from NW Kamyaran and dikes (from a dike complex) and lavas from SE Kamyaran. These are equivalent to the Walash-Naopurdan series of Iraq and the Kamyran series of Iran. Pillow lavas have slight LREE-enriched patterns ($La_{(n)}/Yb_{(n)}$=1.6-1.8), with modest Nb-Ta depletion relative to LREEs ($Nb_{(n)}/La_{(n)}$= 1.2-1.4, Fig. 4a). They are geochemically similar to E-MORB and OIB. Gabbros also have flat to slightly LREE-fractionated patterns with $La_{(n)}/Yb_{(n)}$=0.7-1.5. Depletion in Nb is conspicuous ($Nb_{(n)}/La_{(n)}$=0.5-0.8). Granitic dikes are also enriched in LREE relative to HREE ($La_{(n)}/Yb_{(n)}$=1.8-3.3) and are depleted in Nb-Ta (e.g., $Nb_{(n)}/La_{(n)}$= 0.4-0.8; Fig. 2A). SE Kamyaran lavas and dikes show flat to enriched LREE patterns ($La_{(n)}/Yb_{(n)}$=1.2-24.3), with or without Nb-Ta depletion ($Nb_{(n)}/La_{(n)}$=0.3-1).

ACCEPTED MANUSCRIPT

Downloaded from http://jgs.lyellcollection.org/ at Helmholtz-Zentrum fur Ozeanforschung Kiel on May 28, 2020

Initial εNd ranges from +6.5 to +8.9 for Paleogene magmatic rocks from NW Kamyaran. Their $^{206}Pb/^{204}Pb$ and $^{208}Pb/^{204}Pb$ values change from 18.21 to 19.46 and 38.09 to 40.77, respectively. $^{207}Pb/^{204}Pb$ values range from 15.49 to 15.66. SE Kamyaran dikes and lavas have more variable εNd values; +6.9 to –5.3. Their $^{206}Pb/^{204}Pb$ and $^{208}Pb/^{204}Pb$ values vary from 18.54 to 18.86 and 38.58 to 39.19, respectively. All Paleogene rocks plot above the NHRL on the $^{207}Pb/^{204}Pb$ and $^{208}Pb/^{204}Pb$ versus $^{206}Pb/^{204}Pb$ diagram. SE Kamyaran magmatic rocks show higher involvement of sediments in their mantle source and/or contribution of Iranian continental crust- compared to the NW Kamyaran mafic rocks- although granites from NW Kamyaran have high Pb isotopes. The Pb isotopic composition of Paleogene samples lies between Zagros ophiolites and UDMB igneous rocks (Fig. 4c-d).

Discussion

Paleogene samples have MORB-like to arc-like geochemical signatures, which is shown by variable depletion in Nb-Ta and enrichment in large ion lithophile elements such as Th, U and Ba. In the Th/Yb *vs* Nb/Yb plot (Leat et al. 2004), pillow lavas and some massive lavas plot near the mantle array and are similar to MORBs. Dikes, gabbros and granitic dikes as well as most lavas show higher Th/Yb ratios and are similar to calc-alkaline rocks and arc tholeiites (Fig. 5a). In the field, MORB-like rocks seem to be younger than arc-related rocks. A plot of εNd(t) *vs* Sm/Nd (Fig. 5b) indicates that both depleted mantle similar to the source for N-MORBs and a variety of slab components similar to IBM sediments and/or Cadomian continental crust of Iran were involved in magma genesis. SE Kamyaran dikes have less radiogenic Nd isotopes and lower Sm/Nd ratios compared to pillow lavas and gabbros. Samples with negative εNd(t) and εHf(t) values may reflect melting of a source with mixed proportions of sediment melts and depleted mantle-wedge materials, or contributions of continental crust.

Our new zircon U-Pb ages confirm Eocene ages for magmatic rocks from NW and SE Kamyaran and rule out the Permian-Triassic Gondwana rifting model to generate these rocks. Field evidence shows that Paleogene melts were injected into Late Cretaceous Zagros forearc ophiolites. Paleogene igneous rocks formed in a deep oceanic basin, represented by a thick pile (>1000m) of pillow lavas and interlayered pelagic siliceous sediments. NW Kamyaran preserves tilted, quasi-continuous exposures of oceanic crust where complementary lower and upper crust is exposed. No mantle rocks are exposed with these, and for this reason the Paleogene oceanic crust is not considered to be an ophiolite. It has been suggested that these rocks manifest a Paleogene intra-oceanic arc and back-arc (Ali et al. 2013; Whitechurch et al. 2013), but this is inconsistent with the observation that the Paleogene oceanic realm formed in a forearc setting. A complex scenario calling for an intra-oceanic arc with a back-arc basin to have co-existed with a continental arc on Iranian crust (the UDMB) - with two subduction systems operating at the same time- is unnecessarily complex. It is also geodynamically and geophysically inconsistent with seismic and mantle tomography data that are

ACCEPTED MANUSCRIPT

Downloaded from http://jgs.lyellcollection.org/ at Helmholtz-Zentrum fur Ozeanforschung Kiel on May 28, 2020

most consistent with a single, N-dipping subduction zone (e.g., Al-Lazki et al. 2004; Molinaro et al. 2005; Entezar-Saadat et al. 2017 and references therein).

Continental collision and slab breakoff scenarios are more useful to explain the formation of Miocene UDMB adakitic magmas since there are several lines of evidence- including tectonics- that the collision between Iran and Arabia began ~25 Ma, during the Late Oligocene (McQuarrie & van Hinsbergen 2013; Barber et al. 2018). Apatite (U- Th)/He cooling ages of ~20 Ma from core complex of central Iran further suggest an early Miocene period of north-south shortening related to Late Oligocene collision (Verdel et al. 2007). However, there is also evidence for initial collision between Arabia and Eurasia (including Iran) beginning ~34 Ma (Allen & Armstrong 2008).

We agree that formation of the Paleogene oceanic realm along the Iran-Iraq border was related to a phase of hyperextension. Strong evidence for Paleogene extension is shown elsewhere in the UDMB, producing numerous arc-related extensional basins and core complexes in the upper plate of the Neotethyan subduction zone (Fig. 1a). Paleogene extension was also responsible for forming basins behind the UDMB with thick sequences of volcano-sedimentary rocks, such as those in N and NE Iran (Vincent et al. 2005; Verdel et al. 2011; Sepidbar et al. 2019). There is an age correlation between Paleogene magmatism along the Iran-Iraq border with a peak at *ca* 37 Ma and magmatism in UDMB which started at *ca* 50 Ma onward (Fig. 6). These ages also overlap with those of magmatic rocks from back-arc basins in N and NE Iran (Moghadam et al. 2020a). Strong extension of Iran continental crust may also have caused Paleogene high-flux magmatism in the UDMB (Verdel et al. 2011; Moghadam et al. 2018; Sepidbar et al. 2019). One of these basins, including the WNK basin(s) along the Iraq-Iran border, rifted sufficiently to form new oceanic lithosphere.

Zircon Hf-O and bulk rock Nd isotope composition of some WNK igneous rocks show derivation from more depleted mantle (εHf(t) ~+15, εNd(t) ~+7, δ^{18}O ~+5.5) than that responsible for UDMB arc magmatism (εHf(t) ~+9, εNd(t) ~+3; δ^{18}O ~+6.5) (Fig. 7). These isotopic signatures are similar to those of Late Cretaceous Zagros ophiolites except for SE Kamyaran lavas and dikes which show probable involvement of Iran continental crust. Paleogene forearc rifting to form the WNK basin(s) could reflect weakening of the Iran forearc lithosphere due to slab-released fluids and melts (Baitsch-Ghirardello et al. 2014). This also explains the occurrence of older magmatic rocks (*ca* 40-39 Ma) with trace of extreme contribution of sediment melts and fluids (Fig. 5A). Resolving the subduction contribution for SE Kamyran magmas from trace elements is complicated by isotopic evidence that the edge of Iran Ediacaran-Early Neoproterozoic crust was involved in magma-genesis. Younger rocks (*ca* 36 Ma) with MORB-like signatures were likely generated due to decompression of upwelling mantle beneath the rift with minor contribution of slab-derived fluids, arguing against an important role for hydrous weakening of the lithosphere. Regardless, the forearc rifting scenario we prefer is similar to that documented for the SW Mariana forearc rift, where the Izu-Bonin-Mariana convergent margin experienced forearc rifting ~2 Ma years ago (Ribeiro et al. 2013). In the SE Mariana forearc rift strong regional extension caused MORB- type melts to disrupt Eocene boninitic

ACCEPTED MANUSCRIPT

Downloaded from http://jgs.lyellcollection.org/ at Helmholtz-Zentrum fur Ozeanforschung Kiel on May 28, 2020

and arc tholeiitic crust. This evolution is very is similar to that of the Zagros Paleogene forearc rift. There are two significant differences: 1) in Iran continental crust was involved whereas Mariana rifting only involved oceanic lithosphere; and 2) the Mariana forearc rift cut across the forearc perpendicular to the trench whereas the Iran forearc rift was parallel to forearc and trench.

Trace of other Paleogene oceanic basin(s) may exist elsewhere to the SE in Iran and/or toward the NW, in SE Turkey, wherever the Late Cretaceous forearc suffered extreme extension during Paleogene. Further studies are needed to understand the age and geochemistry of such sequences, e.g., in the Neyriz ophiolite where younger volcanic rocks and sediments known as Hassan-Abad complex are present (Babaie et al. 2001).

Conclusions

Paleogene magmatic rocks including gabbros, granites, dikes and overlying pillow lavas are present in the Iran-Iraq border region, in a >220 km long belt from SE of Kermanshah (Iran) to Hasanbag (Iraq). These igneous rocks are accompanied by and/or interlayered with Paleogene sandstones and pelagic limestones. Field observations indicate that Paleogene rocks were injected into and/or underlain by Late Cretaceous Zagros forearc ophiolites, the Kurdistan-Kermanshah ophiolites. Paleogene igneous rocks show MORB to arc-like geochemical signatures. Zircon U-Pb results show crystallization ages of *ca* 40-37 Ma for these rocks. We believe that a phase of Paleogene hyperextension in the Iranian Plateau- the main triggers for core complex exhumation and high flux magmatism in the UDMB- was also responsible for forming the Paleogene forearc rift that is now preserved along the Iran-Iraq border.

Acknowledgments

This study was funded by the "National Key Research and Development Program of China (2016YFE0203000)" and by "Chinese Academy of Sciences, President's International Fellowship Initiative (PIFI, 2019VCB0013)". We are very grateful to Mark Allen and two anonymous reviewers for their constructive reviews of the manuscript. Editorial suggestions by Tyrone Rooney are also appreciated. We are also very grateful to Y. Liu, X.X. Ling, J. Li, G. Tang, Y.H. Yang, X. Yan and D. Zhang (IGG-CAS) for their assistance during zircon SIMS and LA-ICPMS dating and O isotope, LA-MC-ICPMS Lu-Hf isotope and SEM analyses. All logistical support for the field work came from Damghan University-Iran. This is UTD Geosciences contribution # 13xx.

Figure captions

Figure 1- (a) Geological map of Iran and environs showing Paleogene magmatic and sedimentary rocks and Late Cretaceous ophiolites. (b) Simplified map showing the distribution of Late Cretaceous forearc ophiolites and Paleogene oceanic rocks (Walash- Naopurdan-Kamyran series) along the Iran-Iraq border (modified after (Ali et al. 2013)). Numbers refer to ages in Ma. (c) Geological map of

ACCEPTED MANUSCRIPT

Downloaded from http://jgs.lyellcollection.org/ at Helmholtz-Zentrum fur Ozeanforschung Kiel on May 28, 2020

Paleogene magmatic and sedimentary sequences along the Iran-Iraq border showing the location of dated samples. Numbers refer to ages in Ma. A-B line shows the cross-section position in Fig. 1d. (d) Schematic cross section showing the relations between the Paleogene intrusions and older lithological units (modified after Agard et al. 2005).

Figure 2- (a) Outcrop of Paleogene pillow lavas from SE Kamyaran. (b) Contact between dacitic dikes and (basaltic-) andesitic dikes from SE Kamyaran. (c) Paleogene gabbros in NW Kamyaran. (d) Granitic dikes injected into gabbros. (e) Gabbro inclusions within the overlying pillow lavas- at the contact between gabbros and pillow lavas. (f) and (g) Outcrops of NW Kamyaran pillow lavas.

Figure 3- Zircon LA-ICPMS and SIMS U-Pb plots for Paleogene magmatic rocks.

Figure 4- (a) N-MORB normalized multi-elements patterns for analyzed Paleogene igneous rocks. (b) Evolution plots of zircon Lu-Hf isotope composition of Paleogene rocks, Zagros ophiolites and UDMB-related rocks. CHUR= chondrite normalized uniform reservoir; Depleted mantle array is based on data from modern Mid-Oceanic Ridge basalts with $^{176}Hf/^{177}Hf$=0.28325 and using $^{176}Lu/^{177}Hf$=0.0384 (Chauvel & Blichert-Toft 2001a)). Note that NW Kamyran igneous have more radiogenic Hf isotopic compositions than other Cenozoic igneous rocks from Iran. (c) $^{207}Pb/^{204}Pb$ *vs* $^{206}Pb/^{204}Pb$ and (d) $^{208}Pb/^{204}Pb$ *vs* $^{206}Pb/^{204}Pb$ for Paleogene magmatic rocks. The composition of the mantle components EM-1 and EM-2 are from (Zindler & Hart 1986), whereas composition of subducted sediments is from (Plank & Langmuir 1998). MORB and crust data are from (Nowell et al. 1998; Pearce et al. 1999; Chauvel & Blichert-Toft 2001b; Woodhead et al. 2001). NHRL is after (Vervoort & Blichert-Toft 1999). Published bulk rock Pb isotopes for UDMB and Zagros ophiolites are from (Moghadam et al. 2013b; Moghadam et al. 2014; Sepidbar et al. 2019).

Figure 5- (a) Th/Yb *vs* Nb/Yb plot for Paleogene rocks. Deviations above the mantle array are attributed to addition of subduction components or continental crust assimilation (dashed lines indicate the percent added) (Pearce et al. 1995). (b) εNd(t) *vs* Sm/Nd plot showing that most studied samples have sources that are more similar to Late Cretaceous ophiolites than UDMB igneous rocks. Data for IBM and pelagic sediments are from (Yogodzinski et al. 2018). The composition of continental crust of Iran is from (Moghadam et al. 2020b). Published zircon U-Pb-Hf and bulk rock data for UDMB and Zagros ophiolites are from (Chiu et al. 2013; Moghadam et al. 2016; Chiu et al. 2017; Hosseini et al. 2017; Moghadam et al. 2017; Kazemi et al. 2019; Sepidbar et al. 2019). For comparison, we also show the composition of Paleogene rocks from SE Kamyaran and Kermanshah (Azizi et al. 2011b; Nouri et al. 2017).

ACCEPTED MANUSCRIPT

Downloaded from http://jgs.lyellcollection.org/ at Helmholtz-Zentrum fur Ozeanforschung Kiel on May 28, 2020

Figure 6- Histograms showing the magmatic age distribution of (a) Walash- Naopurdan-Kamyran (WNK) series igneous rocks (-yellow) and Zagros Late Cretaceous ophiolites (-blue), and (b) UDMB magmatic rocks. Zagros ophiolites are as old as *ca* 110 Ma with a peak at *ca* 98 Ma (a). Magmatic rocks along the Iran-Iraq border show magmatic climax at *ca* 37, indistinguishable from the UDMB magmatic climax. Published zircon U-Pb data from Iran are from (Chiu et al. 2013; Moghadam et al. 2016; Chiu et al. 2017; Hosseini et al. 2017; Moghadam et al. 2017; Kazemi et al. 2019; Sepidbar et al. 2019).

Figure 7- Histograms showing zircon Hf-O and bulk rock Nd isotopic composition of magmatic rocks from Walash-Naopurdan-Kamyran (WNK) igneous rocks, Zagros ophiolites and UDMB magmatic rocks. UDMB rocks have evolved zircon Hf-O and bulk rock Nd isotopic signature than Paleogene rocks except some older magmatic rocks (*ca* 40-39 Ma) with trace of involvement of old continental crust of Iran. References for published zircon Hf-O and bulk rock Nd data for Zagros ophiolites and UDMB are similar to figures 5 and 6.

Figure 8- Simplified cross-section of the Paleogene convergent margin of Iran, emphasizing extreme extension in the Iranian plateau during Paleogene (50-35 Ma). This figure also indicates the positions of the forearc rift, Urumieh-Dokhtar Magmatic Belt (UDMB), back-arc magmatism and core complex. Small wavy red lines show the trajectory of slab fluids whereas continuous red line shows the asthenosphere mantle flow.

ACCEPTED MANUSCRIPT

Downloaded from http://jgs.lyellcollection.org/ at Helmholtz-Zentrum fur Ozeanforschung Kiel on May 28, 2020

References

Agard, P., Omrani, J., Jolivet, L. & Mouthereau, F. 2005. Convergence history across Zagros (Iran): constraints from collisional and earlier deformation. *International Journal of Earth Sciences*, **94**, 401-419.

Al-Lazki, A.I., Sandvol, E., Seber, D., Barazangi, M., Turkelli, N. & Mohamad, R. 2004. Pn tomographic imaging of mantle lid velocity and anisotropy at the junction of the Arabian, Eurasian and African plates. *Geophysical Journal International*, **158**, 1024-1040, http://doi.org/DOI 10.1111/j.1365-246X.2004.02355.x.

Ali, S.A., Buckman, S., Aswad, K.J., Jones, B.G., Ismail, S.A. & Nutman, A.P. 2013. The tectonic evolution of a Neo- Tethyan (Eocene–Oligocene) island- arc (Walash and Naopurdan groups) in the Kurdistan region of the Northeast Iraqi Zagros Suture Zone. *Island Arc*, **22**, 104-125.

Allen, M.B. & Armstrong, H.A. 2008. Arabia–Eurasia collision and the forcing of mid-Cenozoic global cooling. *Palaeogeography, Palaeoclimatology, Palaeoecology*, **265**, 52-58.

Ao, S., Xiao, W., Jafari, M.K., Talebian, M., Chen, L., Wan, B., Ji, W. & Zhang, Z. 2016. U–Pb zircon ages, field geology and geochemistry of the Kermanshah ophiolite (Iran): From continental rifting at 79 Ma to oceanic core complex at ca. 36 Ma in the southern Neo-Tethys. *Gondwana Research*, **31**, 305-318.

Aswad, K.J. 1999. Arc-continent collision in Northeastern Iraq as evidenced by Mawat and Penjwin Ophiolite Complexes. *Raffidain Journal of Science*, **10**, 51-61.

Aswad, K.J., Aziz, N.R. & Koyi, H.A. 2011. Cr-spinel compositions in serpentinites and their implications for the petrotectonic history of the Zagros Suture Zone, Kurdistan Region, Iraq. *Geological Magazine*, **148**, 802-818.

Aswad, K.J.A., Al-Samman, A.H.M., Aziz, N.R.H. & Koyi, A.M.A. 2014. The geochronology and petrogenesis of Walash volcanic rocks, Mawat nappes: constraints on the evolution of the northwestern Zagros suture zone, Kurdistan Region, Iraq. *Arabian Journal of Geosciences*, **7**, 1403-1432.

Aziz, N.R., Elias, E.M. & Aswad, K.J.A. 2011a. Rb–Sr and Sm–Nd isotope study of serpentinites and their impact on the tectonic setting of Zagros Suture Zone, NE-Iraq. *Iraqi Bulletin of Geology and Mining*, **7**, 67-75.

Aziz, N.R.H., Aswad, K.J.A. & Koyi, H.A. 2011b. Contrasting settings of serpentinite bodies in the northwestern Zagros Suture Zone, Kurdistan Region, Iraq. *Geological Magazine*, **148**, 819-837.

Azizi, H., Tanaka, T., Asahara, Y., Chung, S.L. & Zarrinkoub, M.H. 2011a. Discrimination of the age and tectonic setting for magmatic rocks along the Zagros thrust zone, northwest Iran, using the zircon U–Pb age and Sr–Nd isotopes. *Journal of Geodynamics*, **52**, 304-320, http://doi.org/http://dx.doi.org/10.1016/j.jog.2011.03.001.

Azizi, H., Tanaka, T., Asahara, Y., Chung, S.L. & Zarrinkoub, M.H. 2011b. Discrimination of the age and tectonic setting for magmatic rocks along the Zagros thrust zone, northwest Iran, using the zircon U-Pb age and Sr-Nd isotopes. *Journal of Geodynamics*, **52**, 304-320.

Babaei, A., Babaie, H.A. & Arvin, M. 2005. Tectonic evolution of the Neyriz ophiolite, Iran: An accretionary prism model. *Ofioliti*, **30**, 65-74.

ACCEPTED MANUSCRIPT

Downloaded from http://jgs.lyellcollection.org/ at Helmholtz-Zentrum fur Ozeanforschung Kiel on May 28, 2020

Babaie, H.A., Babaei, A., Ghazi, A.M. & Arvin, M. 2006. Geochemical, Ar-40/Ar-39 age, and isotopic data for crustal rocks of the Neyriz ophiolite, Iran. *Canadian Journal of Earth Sciences*, **43**, 57-70.

Babaie, H.A., Ghazi, A.M., Babaei, A., La Tour, T.E. & Hassanipak, A.A. 2001. Geochemistry of are volcanic rocks of the Zagros Crush Zone, Neyriz, Iran. *Journal of Asian Earth Sciences*, **19**, 61-76.

Baitsch-Ghirardello, B., Gerya, T.V. & Burg, J.-P. 2014. Geodynamic regimes of intra-oceanic subduction: Implications for arc extension vs. shortening processes. *Gondwana Research*, **25**, 546-560.

Barber, D.E., Stockli, D.F., Horton, B.K. & Koshnaw, R.I. 2018. Cenozoic Exhumation and Foreland Basin Evolution of the Zagros Orogen During the Arabia-Eurasia Collision, Western Iran. *Tectonics*, **37**, 4396-4420, http://doi.org/10.1029/2018tc005328.

Chauvel, C. & Blichert-Toft, J. 2001a. A hafnium isotope and trace element perspective on melting of the depleted mantle. *Earth and Planetary Science Letters*, **190**, 137-151.

Chauvel, C. & Blichert-Toft, J. 2001b. A hafnium isotope and trace element perspective on melting of the depleted mantle. *Earth and Planetary Science Letters*, **190**, 137-151.

Chauvet, F., Lapierre, H., Maury, R.C., Bosch, D., Basile, C., Cotten, J., Brunet, P. & Campillo, S. 2011. Triassic alkaline magmatism of the Hawasina Nappes: Post-breakup melting of the Oman lithospheric mantle modified by the Permian Neotethyan Plume. *Lithos*, **122**, 122-136.

Chiu, H.Y., Chung, S.L., Zarrinkoub, M.H., Mohammadi, S.S., Khatib, M.M. & Iizuka, Y. 2013. Zircon U-Pb age constraints from Iran on the magmatic evolution related to Neotethyan subduction and Zagros orogeny. *Lithos*, **162**, 70-87, http://doi.org/10.1016/j.lithos.2013.01.006.

Chiu, H.Y., Chung, S.L., Zarrinkoub, M.H., Melkonyan, R., Pang, K.N., Lee, H.Y., Wang, K.L., Mohammadi, S.S., *et al*. 2017. Zircon Hf isotopic constraints on magmatic and tectonic evolution in Iran: Implications for crustal growth in the Tethyan orogenic belt. *Journal of Asian Earth Sciences*, **145**, 652-669, http://doi.org/10.1016/j.jseaes.2017.06.011.

Dilek, Y. & Thy, P. 2009. Island arc tholeiite to boninitic melt evolution of the Cretaceous Kizildag (Turkey) ophiolite: Model for multi-stage early arc-forearc magmatism in Tethyan subduction factories. *Lithos*, **113**, 68-87.

Dilek, Y. & Altunkaynak, S. 2010. Geochemistry of Neogene-Quaternary alkaline volcanism in western Anatolia, Turkey, and implications for the Aegean mantle. *International Geology Review*, **52**, 631-655.

Dilek, Y., Furnes, H. & Shallo, M. 2007. Suprasubduction zone ophiolite formation along the periphery of Mesozoic Gondwana. *Gondwana Research*, **11**, 453-475, http://doi.org/10.1016/j.gr.2007.01.005.

Dilek, Y., Imamverdiyev, N. & Altunkaynak, S. 2010. Geochemistry and tectonics of Cenozoic volcanism in the Lesser Caucasus (Azerbaijan) and the peri-Arabian region: collision-induced mantle dynamics and its magmatic fingerprint. *International Geology Review*, **52**, 536-578, http://doi.org/Pii 916753443
Doi 10.1080/00206810903360422.

Entezar-Saadat, V., Motavalli-Anbaran, S.-H. & Zeyen, H. 2017. Lithospheric structure of the Eastern Iranian plateau from integrated geophysical modeling: A transect from Makran to the Turan platform. *Journal of Asian Earth Sciences*, **138**, 357-366, http://doi.org/10.1016/j.jseaes.2017.02.024.

ACCEPTED MANUSCRIPT

Downloaded from http://jgs.lyellcollection.org/ at Helmholtz-Zentrum fur Ozeanforschung Kiel on May 28, 2020

Ghazi, J.M., Moazzen, M., Rahgoshay, M. & Moghadam, H.S. 2010. Mineral chemical composition and geodynamic significance of peridotites from Nain ophiolite, central Iran. *Journal of Geodynamics*, **49**, 261-270.

Golonka, J. 2004. Plate tectonic evolution of the southern margin of Eurasia in the Mesozoic and Cenozoic. *Tectonophysics*, **381**, 235-273, http://doi.org/10.1016/j.tecto.2002.06.004.

Hassan, M.M., Jones, B.G., Buckman, S., Al Jubory, A.I. & Ismail, S.A. 2015. Source area and tectonic provenance of Paleocene–Eocene red bed clastics from the Kurdistan area NE Iraq: Bulk-rock geochemistry constraints. *Journal of African Earth Sciences*, **109**, 68-86.

Hosseini, M.R., Hassanzadeh, J., Alirezaei, S., Sun, W.D. & Li, C.Y. 2017. Age revision of the Neotethyan arc migration into the southeast Urumieh-Dokhtar belt of Iran: Geochemistry and U-Pb zircon geochronology. *Lithos*, **284**, 296-309, http://doi.org/10.1016/j.lithos.2017.03.012.

Ishizuka, O., Tani, K. & Reagan, M.K. 2014. Izu-Bonin-Mariana Forearc Crust as a Modern Ophiolite Analogue. *Elements*, **10**, 115-120, http://doi.org/10.2113/gselements.10.2.115.

Kazemi, Z., Ghasemi, H., Tilhac, R., Griffin, W., Moghadam, H.S., O'Reilly, S. & Mousivand, F. 2019. Late Cretaceous subduction-related magmatism on the southern edge of Sabzevar basin, NE Iran. *Journal of the Geological Society*, **176**, 530-552, http://doi.org/10.1144/jgs2018-076.

Leat, P.T., Pearce, J.A., Barker, P.F., Millar, I.L., Barry, T.L. & Larter, R.D. 2004. Magma genesis and mantle flow at a subducting slab edge: the South Sandwich arc-basin system. *Earth and Planetary Science Letters*, **227**, 17-35, http://doi.org/10.1016/j.epsl.2004.08.016.

Mazhari, S.A., Bea, F., Amini, S., Ghalamghash, J., Molina, J.F., Montero, P., Scarrow, J.H. & Williams, I.S. 2009. The Eocene bimodal Piranshahr massif of the Sanandaj–Sirjan Zone, NW Iran: a marker of the end of the collision in the Zagros orogen. *Journal of the Geological Society*, **166**, 53-69, http://doi.org/10.1144/0016-76492008-022.

McQuarrie, N. & van Hinsbergen, D.J.J. 2013. Retrodeforming the Arabia-Eurasia collision zone: Age of collision versus magnitude of continental subduction. *Geology*, **41**, 315-318.

Moghadam, H.S. & Stern, R.J. 2011. Geodynamic evolution of Upper Cretaceous Zagros ophiolites: formation of oceanic lithosphere above a nascent subduction zone. *Geological Magazine*, **148**, 762-801.

Moghadam, H.S. & Stern, R.J. 2015. Ophiolites of Iran: Keys to understanding the tectonic evolution of SW Asia: (II) Mesozoic ophiolites. *Journal of Asian Earth Sciences*, **100**, 31-59, http://doi.org/10.1016/j.jseaes.2014.12.016.

Moghadam, H.S., Stern, R.J. & Rahgoshay, M. 2010. The Dehshir ophiolite (central Iran): Geochemical constraints on the origin and evolution of the Inner Zagros ophiolite belt. *Geological Society of America Bulletin*, **122**, 1516-1547, http://doi.org/Doi 10.1130/B30066.1.

Moghadam, H.S., Mosaddegh, H. & Santosh, M. 2013a. Geochemistry and petrogenesis of the Late Cretaceous Haji-Abad ophiolite (Outer Zagros Ophiolite Belt, Iran): implications for geodynamics of the Bitlis-Zagros suture zone. *Geological Journal*, **48**, 579-602, http://doi.org/Doi 10.1002/Gj.2458.

Moghadam, H.S., Stern, R.J., Chiaradia, M. & Rahgoshay, M. 2013b. Geochemistry and tectonic evolution of the Late Cretaceous Gogher-Baft ophiolite, central Iran. *Lithos*, **168**, 33-47, http://doi.org/10.1016/j.lithos.2013.01.013.

ACCEPTED MANUSCRIPT

Downloaded from http://jgs.lyellcollection.org/ at Helmholtz-Zentrum fur Ozeanforschung Kiel on May 28, 2020

Moghadam, H.S., Stern, R.J., Kimura, J.I., Hirahara, Y., Senda, R. & Miyazaki, T. 2012. Hf-Nd isotope constraints on the origin of Dehshir Ophiolite, Central Iran. *Island Arc*, **21**, 202-214.

Moghadam, H.S., Khedr, M.Z., Chiaradia, M., Stern, R.J., Bakhshizad, F., Arai, S., Ottley, C.J. & Tamura, A. 2014. Supra-subduction zone magmatism of the Neyriz ophiolite, Iran: constraints from geochemistry and Sr-Nd-Pb isotopes. *International Geology Review*, **56**, 1395-1412, http://doi.org/10.1080/00206814.2014.942391.

Moghadam, H.S., Rossetti, F., Lucci, F., Chiaradia, M., Gerdes, A., Martinez, M.L., Ghorbani, G. & Nasrabady, M. 2016. The calc-alkaline and adakitic volcanism of the Sabzevar structural zone (NE Iran): Implications for the Eocene magmatic flare-up in Central Iran. *Lithos*, **248**, 517-535, http://doi.org/10.1016/j.lithos.2016.01.019.

Moghadam, H.S., Li, Q.L., Li, X.H., Stern, R.J., Levresse, G., Santos, J.F., Lopez Martinez, M., Ducea, M.N.G., G., *et al*. 2020a. Neotethyan Subduction Ignited the Iran Arc and Backarc Differently. *Journal of Geophysical Research (solid Earth)*, **125**, http://doi.org/10.1029/2019JB018460.

Moghadam, H.S., Li, Q.L., Griffin, W.L., Stern, R.J., Ishizuka, O., Henry, H., Lucci, F., O'Reilly, S.Y., *et al*. 2020b. Repeated magmatic buildup and deep "hot zones" in continental evolution: The Cadomian crust of Iran. *Earth and Planetary Science Letters*, http://doi.org/https://doi.org/10.1016/j.epsl.2019.115989.

Moghadam, H.S., Griffin, W.L., Li, X.H., Santos, J.F., Karsli, O., Stern, R.J., Ghorbani, G., Gain, S., *et al*. 2017. Crustal Evolution of NW Iran: Cadomian Arcs, Archean Fragments and the Cenozoic Magmatic Flare-Up. *Journal of Petrology*, **58**, 2143-2190, http://doi.org/10.1093/petrology/egy005.

Moghadam, H.S., Griffin, W.L., Kirchenbaur, M., Garbe-Schönberg, D., Zakie Khedr, M., Kimura, J.-I., Stern, R.J., Ghorbani, G., *et al*. 2018. Roll-Back, Extension and Mantle Upwelling Triggered Eocene Potassic Magmatism in NW Iran. *Journal of Petrology*, **59**, 1417-1465, http://doi.org/10.1093/petrology/egy067.

Molinaro, M., Zeyen, H. & Laurencin, X. 2005. Lithospheric structure beneath the south-eastern Zagros Mountains, Iran: recent slab break-off? *Terra Nova*, **17**, 1-6, http://doi.org/DOI 10.1111/j.1365-3121.2004.00575.x.

Monsef, I., Monsef, R., Mata, J., Zhang, Z.Y., Pirouz, M., Rezaeian, M., Esmaeili, R. & Xiao, W.J. 2018. Evidence for an early-MORB to fore-arc evolution within the Zagros suture zone: Constraints from zircon U-Pb geochronology and geochemistry of the Neyriz ophiolite (South Iran). *Gondwana Research*, **62**, 287-305, http://doi.org/10.1016/j.gr.2018.03.002.

Nouri, F., Asahara, Y., Azizi, H., Yamamoto, K. & Tsuboi, M. 2017. Geochemistry and petrogenesis of the Eocene-back arc mafic rocks in the Zagros suture zone, northern Noorabad, western Iran. *Chemie Der Erde-Geochemistry*, **77**, 517-533, http://doi.org/10.1016/j.chemer.2017.06.002.

Nouri, F., Azizi, H., Golonka, J., Asahara, Y., Orihashi, Y., Yamamoto, K., Tsuboi, M. & Anma, R. 2016. Age and petrogenesis of Na-rich felsic rocks in western Iran: Evidence for closure of the southern branch of the Neo-Tethys in the Late Cretaceous. *Tectonophysics*, **671**, 151-172, http://doi.org/10.1016/j.tecto.2015.12.014.

Nowell, G., Kempton, P., Noble, S., Fitton, J., Saunders, A., Mahoney, J. & Taylor, R. 1998. High precision Hf isotope measurements of MORB and OIB by thermal ionisation mass spectrometry: insights into the depleted mantle. *Chemical Geology*, **149**, 211-233.

ACCEPTED MANUSCRIPT

Downloaded from http://jgs.lyellcollection.org/ at Helmholtz-Zentrum fur Ozeanforschung Kiel on May 28, 2020

Numan, N.M. 2001. Cretaceous and Tertiary Alpine subductional history in Northern Iraq. *Iraqi J Earth Sci*, **1**, 59-74.

Pearce, J., Kempton, P., Nowell, G. & Noble, S. 1999. Hf-Nd element and isotope perspective on the nature and provenance of mantle and subduction components in Western Pacific arc-basin systems. *Journal of Petrology*, **40**, 1579-1611.

Pearce, J.A., Baker, P.E., Harvey, P.K. & Luff, I.W. 1995. Geochemical Evidence for Subduction Fluxes, Mantle Melting and Fractional Crystallization beneath the South Sandwich-Island Arc. *Journal of Petrology*, **36**, 1073-1109.

Plank, T. & Langmuir, C.H. 1998. The chemical composition of subducting sediment and its consequences for the crust and mantle. *Chemical Geology*, **145**, 325-394.

Ribeiro, J.M., Stern, R.J., Martinez, F., Ishizuka, O., Merle, S.G., Kelley, K., Anthony, E.Y., Ren, M.H., *et al*. 2013. Geodynamic evolution of a forearc rift in the southernmost Mariana Arc. *Island Arc*, **22**, 453-476.

Saccani, E., Allahyari, K. & Rahimzadeh, B. 2014. Petrology and geochemistry of mafic magmatic rocks from the Sarve-Abad ophiolites (Kurdistan region, Iran): Evidence for interaction between MORB-type asthenosphere and OIB-type components in the southern Neo-Tethys Ocean. *Tectonophysics*, **621**, 132-147.

Sepidbar, F., Shafaii Moghadam, H., Zhang, L., Li, J.-W., Ma, J., Stern, R.J. & Lin, C. 2019. Across-arc geochemical variations in the Paleogene magmatic belt of Iran. *Lithos*, **344-345**, 280-296, http://doi.org/10.1016/j.lithos.2019.06.022.

van Hinsbergen, D.J., Maffione, M., Koornneef, L.M. & Guilmette, C. 2019. Kinematic and paleomagnetic restoration of the Semail ophiolite (Oman) reveals subduction initiation along an ancient Neotethyan fracture zone. *Earth and Planetary Science Letters*, **518**, 183-196.

Verdel, C., Wernicke, B.P., Hassanzadeh, J. & Guest, B. 2011. A Paleogene extensional arc flare-up in Iran. *Tectonics*, **30**, http://doi.org/Artn Tc3008 10.1029/2010tc002809.

Verdel, C., Wernicke, B.P., Ramezani, J., Hassanzadeh, J., Renne, P.R. & Spell, T.L. 2007. Geology and thermochronology of Tertiary Cordilleran-style metamorphic core complexes in the Saghand region of central Iran. *Geological Society of America Bulletin*, **119**, 961-977, http://doi.org/Doi 10.1130/B26102.1.

Vervoort, J.D. & Blichert-Toft, J. 1999. Evolution of the depleted mantle: Hf isotope evidence from juvenile rocks through time. *Geochimica Et Cosmochimica Acta*, **63**, 533-556.

Vincent, S.J., Allen, M.B., Ismail-Zadeh, A.D., Flecker, R., Foland, K.A. & Simmons, M.D. 2005. Insights from the Talysh of Azerbaijan into the Paleogene evolution of the South Caspian region. *Geological Society of America Bulletin*, **117**, 1513-1533.

Whitechurch, H., Omrani, J., Agard, P., Humbert, F., Montigny, R. & Jolivet, L. 2013. Evidence for Paleocene–Eocene evolution of the foot of the Eurasian margin (Kermanshah ophiolite, SW Iran) from back-arc to arc: Implications for regional geodynamics and obduction. *Lithos*, **182–183**, 11-32, http://doi.org/http://dx.doi.org/10.1016/j.lithos.2013.07.017.

Woodhead, J., Hergt, J., Davidson, J. & Eggins, S. 2001. Hafnium isotope evidence for 'conservative'element mobility during subduction zone processes. *Earth and Planetary Science Letters*, **192**, 331-346.

ACCEPTED MANUSCRIPT

Downloaded from http://jgs.lyellcollection.org/ at Helmholtz-Zentrum fur Ozeanforschung Kiel on May 28, 2020

Yogodzinski, G.M., Bizimis, M., Hickey-Vargas, R., McCarthy, A., Hocking, B.D., Savov, I.P., Ishizuka, O. & Arculus, R. 2018. Implications of Eocene-age Philippine Sea and forearc basalts for initiation and early history of the Izu-Bonin-Mariana arc. *Geochimica Et Cosmochimica Acta*, **228**, 136-156, http://doi.org/10.1016/j.gca.2018.02.047.

Zindler, A. & Hart, S. 1986. Chemical geodynamics. *Annual Review of Earth and Planetary Sciences*, **14**, 493-571.

ACCEPTED MANUSCRIPT

(a)

200 km

Caspian Sea

Turan Platform

Kopet Dagh

Khoy

Urumieh Lake

Zanjan

Takab

Marivan

Iraq

Kermanshah

Fig. 1B

Golapayegan

Tehran

Urumieh-Dokhtar Magmatic Belt

Torud

Sabzevar

Torbat-e-Heydarieh

Nain

Saghand

Birjand

Dehshir

Zagros Fold-Thrust Belt

Sanandaj-Sirjan Zone

Main Zagros Thrust

Neyriz

Baft

Bam

Haji Abad

Kahnuj

Rameshk

Persian Gulf

Core complex

Paleogene magmatic rocks

Paleogene sedimentary rocks

Late Cretaceous ophiolites

(b)

50 km

MZT

Ali et al., 2013
43.01±0.15

24.10±4.8
Ali et al., 2013

Hasanbag

Qalander

Rayat

43.1±0.3 Ar-Ar dating

35.7±0.5 U-Pb dating

Piranshahr

Pushtashan

Erbil

Sardasht

Bulfat

Zagros Suture Zone

Aswad et al., 2014

Mawat

43.1±0.3
40.1±0.3
32.3±0.4

Penjween

Kirkuk

Soleimanieh

Zagros Fold-Thrust Belt

Sanandaj-Sirjan Zone

IRAQ

Marivan

Sanandaj

Sarve-Abad

Kamyaran

Fig. 1C

Ao et al., 2016
35.7±0.5

Kermanshah

Sahneh

Harsin

Boundary between Iraq & Iran

Main Zagros Thrust

Paleogene presumed "ophiolite"

Walash-Naopurdan-Kamyaran magmatic rocks

Naopurdan volcanosediments

Late Cretaceous ophiolites

Serpentinized peridotites, lavas, pelagic sediments

Continental passive margin sediments

Avroman-Bisotun limestones (Triassic-Cretaceous)

Qulqula-Kermanshah radiolarites (Triassic-Cretaceous)

37°00′

36°00′

35°00′

34°00′

44°00′

45°00′

46°00′

47°00′

(c)

35°45′

35°30′

35°15′

35°00′

46°00′

46°15′

46°30′

47°00′

47°15′

Marivan

Pyazeh

Sanandaj-Sirjan Zone

IRAQ

20 km

This study
39.4±0.1
36.9±0.1

Azizi et al., 2011
39.7±0.5
39.5±0.3

Azizi et al., 2011
54.6±0.3

This study
39.4±0.1

This study
36.9±0.1

Sarve-Abad

Karreh Gol

Kherran

Zagros Fold-Thrust Belt

A

B

Paleogene WNK sequences

Pelagic limestones, volcanosediments

Massive and pillowed lavas

Granites

Gabbros-diorites

Dike complex

(d)

A

B

MZT

~40 Ma

SaSZ

?

10 km

Late Cretaceous ophiolites

Serpentinized peridotites, lavas, pelagic sediments

Continental passive margin sediments

Avroman-Bisotun limestones (Triassic-Cretaceous)

Qulqula-Kermanshah radiolarites (Triassic-Cretaceous)

ACCEPTED MANUSCRIPT

Downloaded from http://gsa.lyellcollection.org/ at Helmholtz-Zentrum fur Ozeanforschung Kiel on May 28, 2020

a

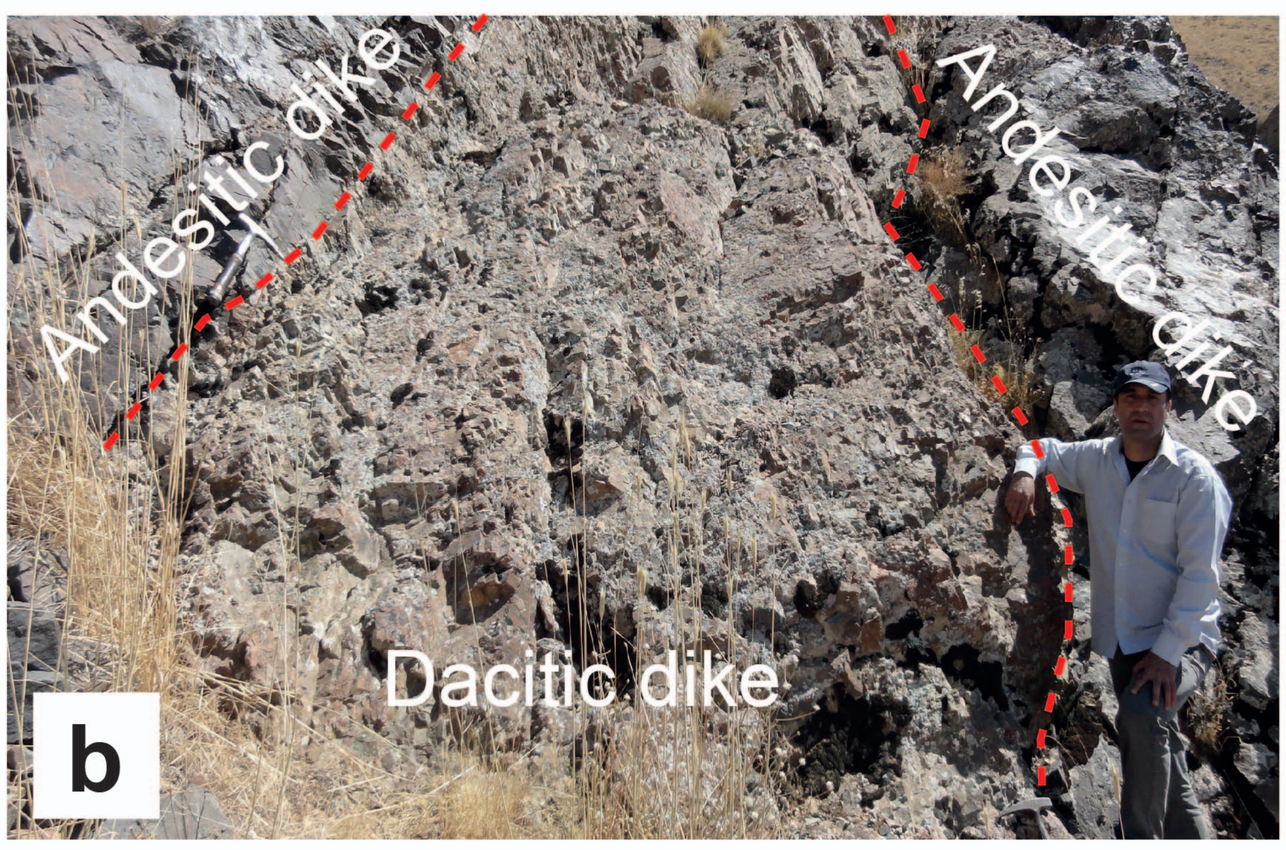

b

c

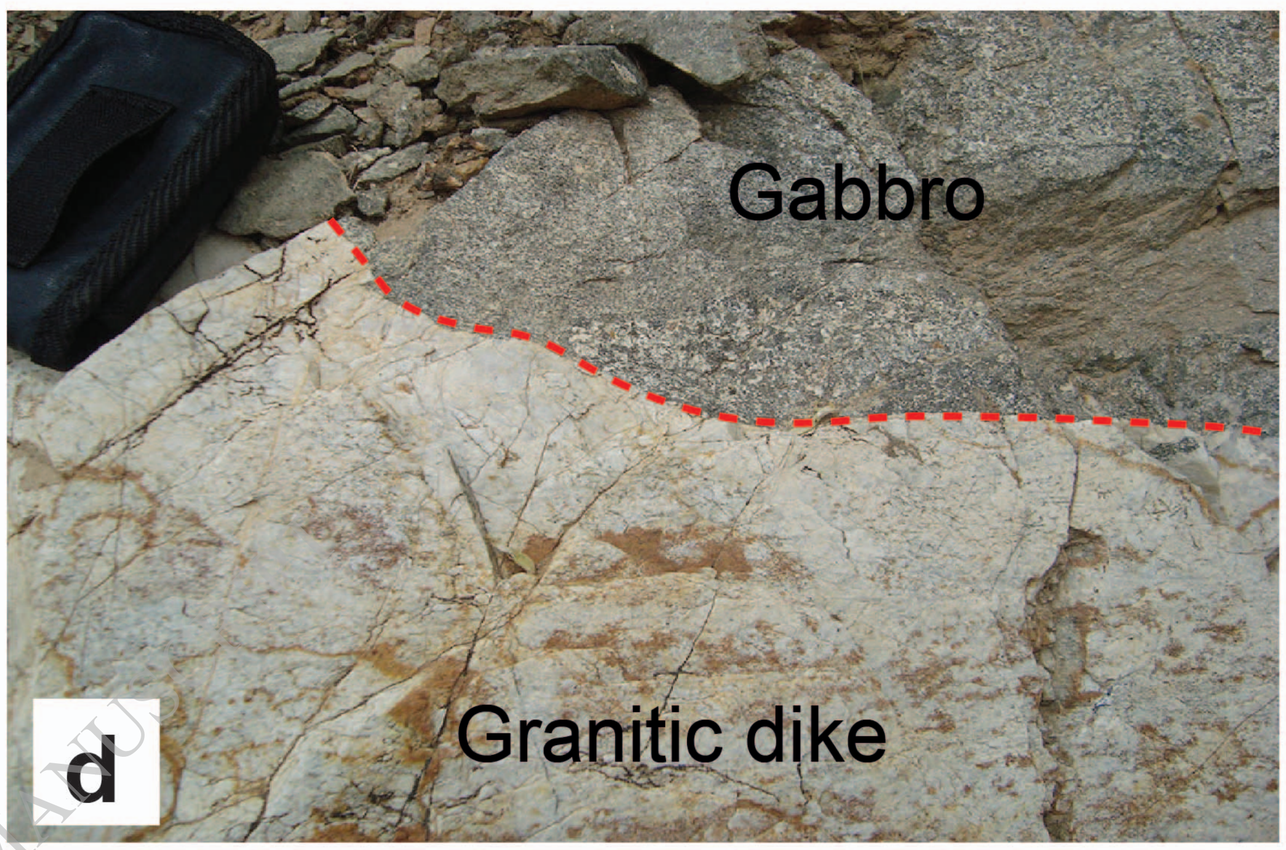

d

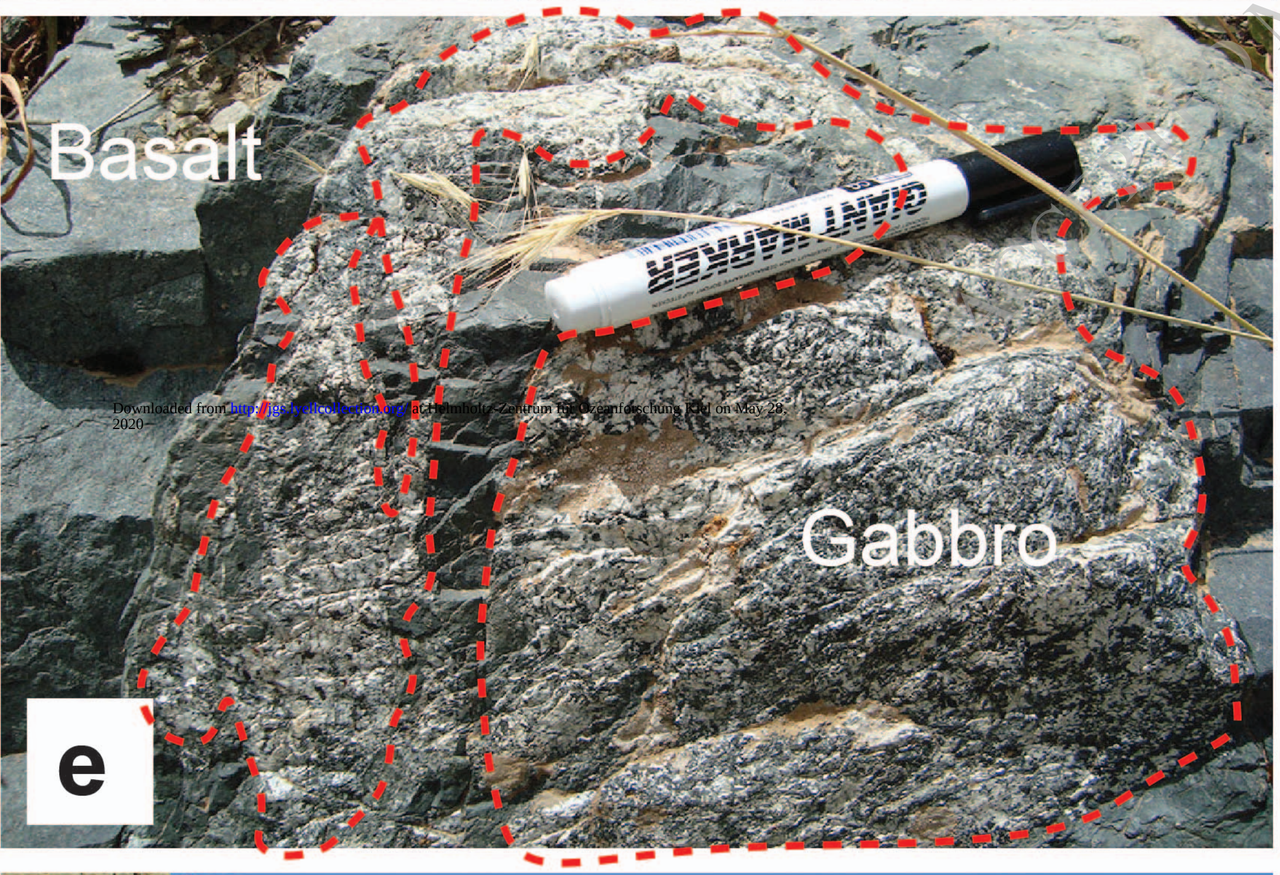

e

Downloaded from http://gsa.geoscienceworld.org/ at Helmholtz-Zentrum für Ozeanforschung Kiel on May 28, 2020

f

g

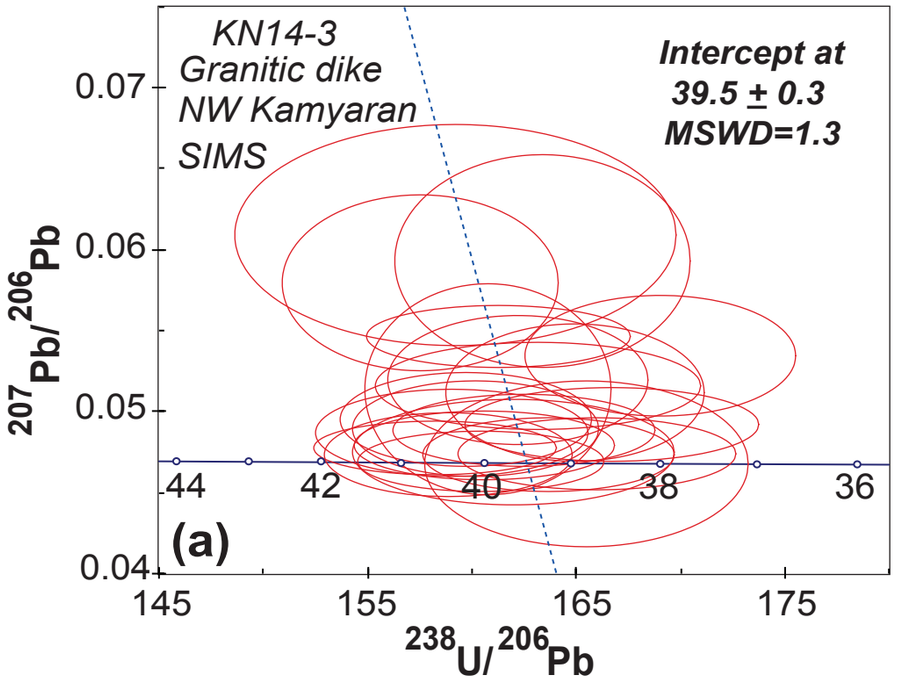

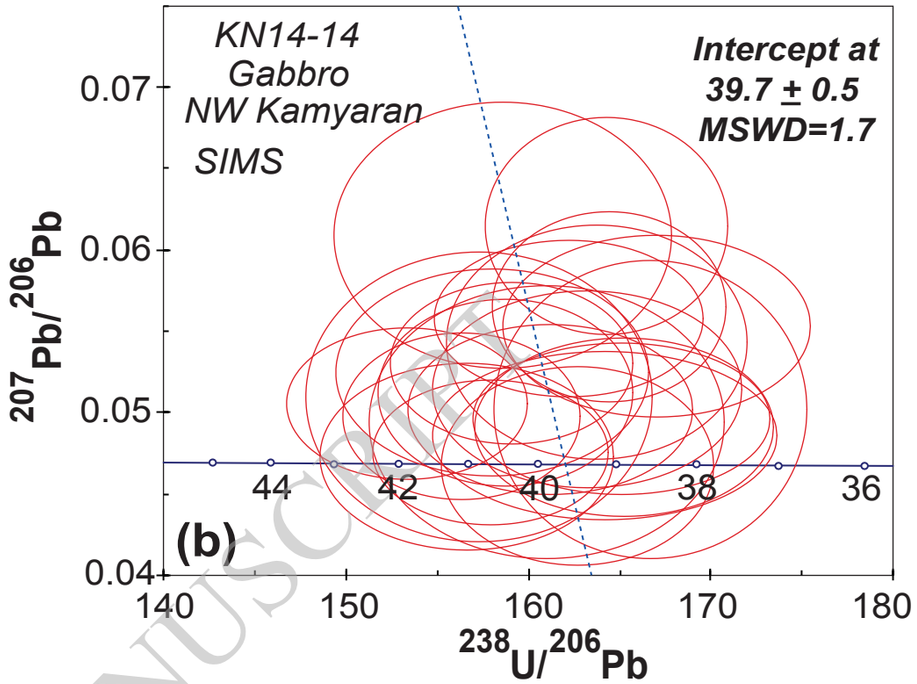

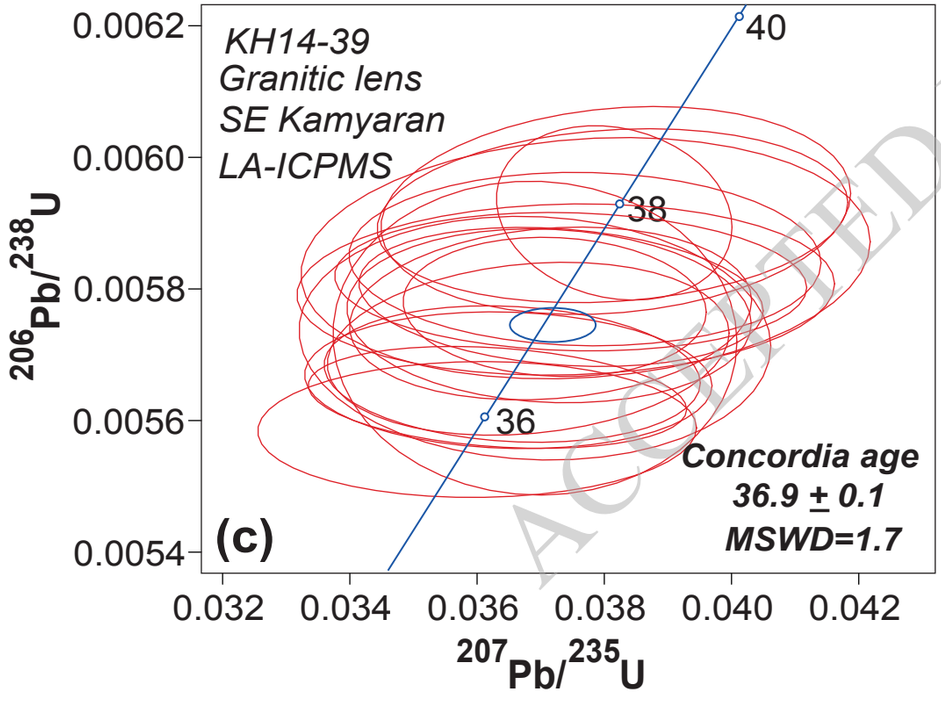

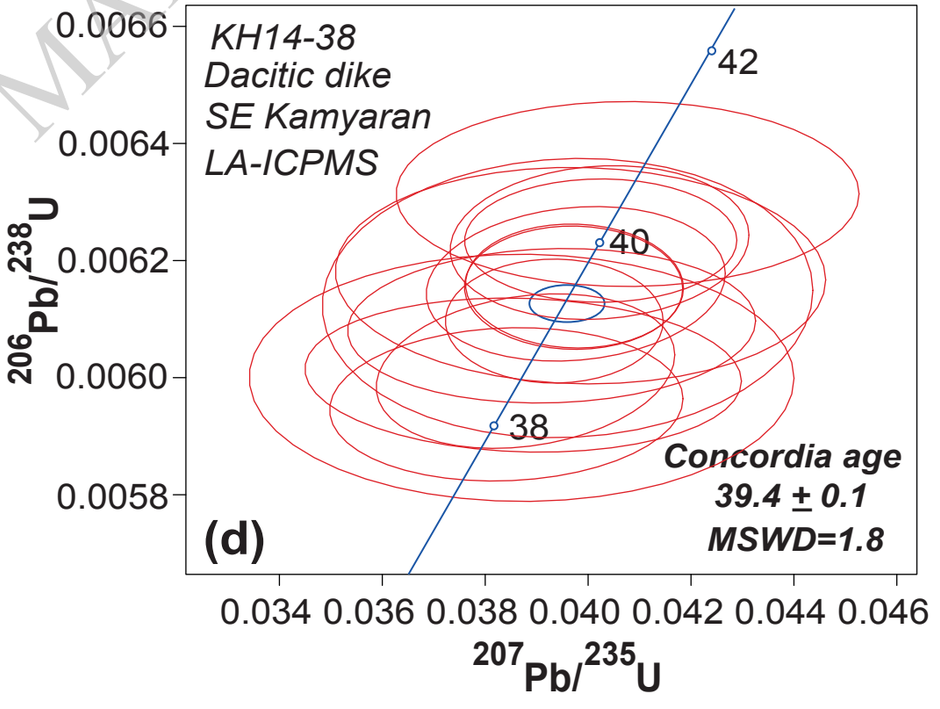

ACCEPTED MANUSCRIPT

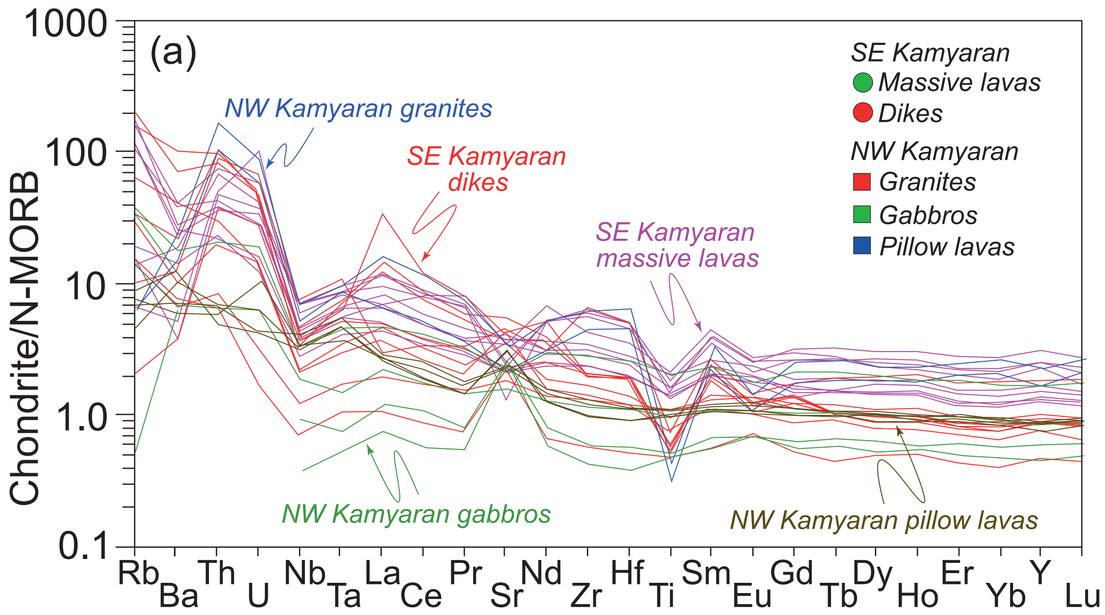

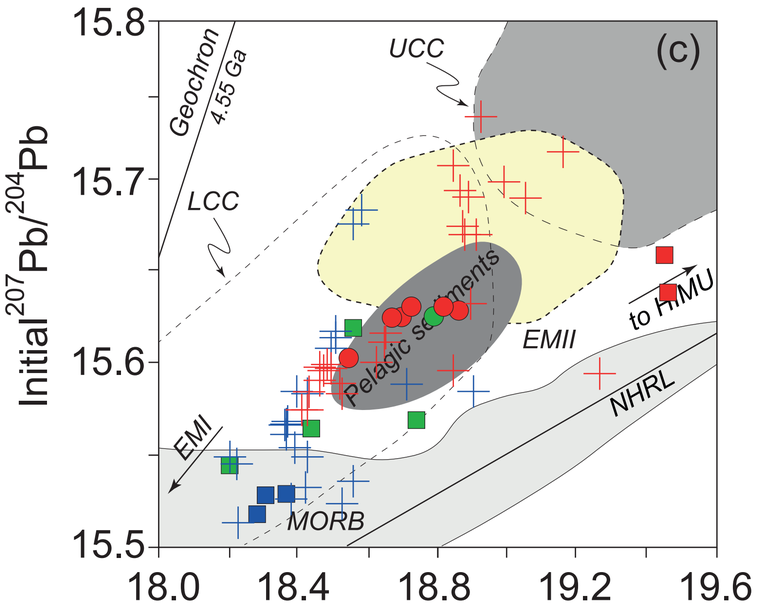

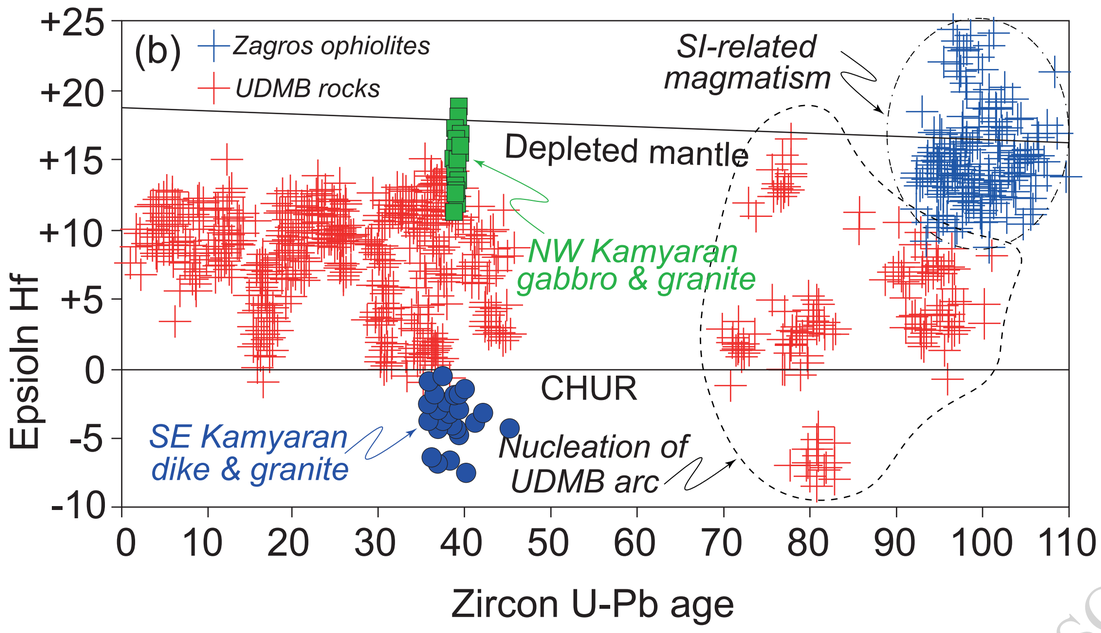

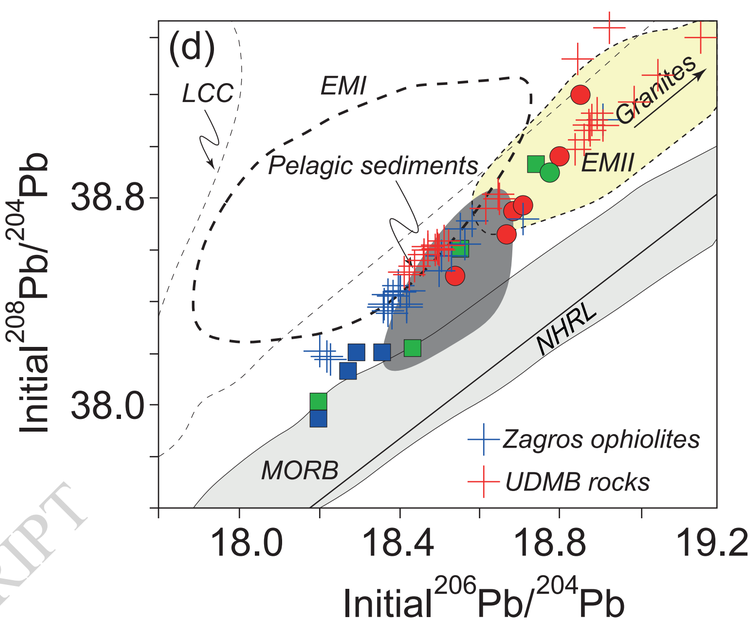

ACCEPTED MANUSCRIPT

Downloaded from http://jgs.lyellcollection.org/ at Helmholtz-Zentrum fur Ozeanforschung Kiel on May 28, 2020

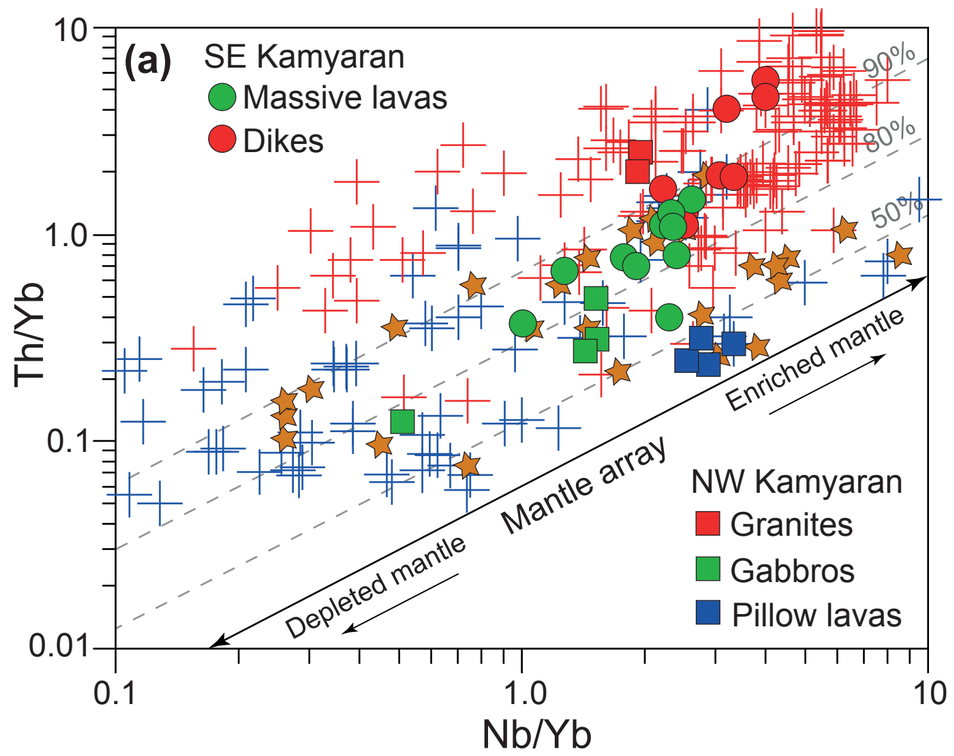

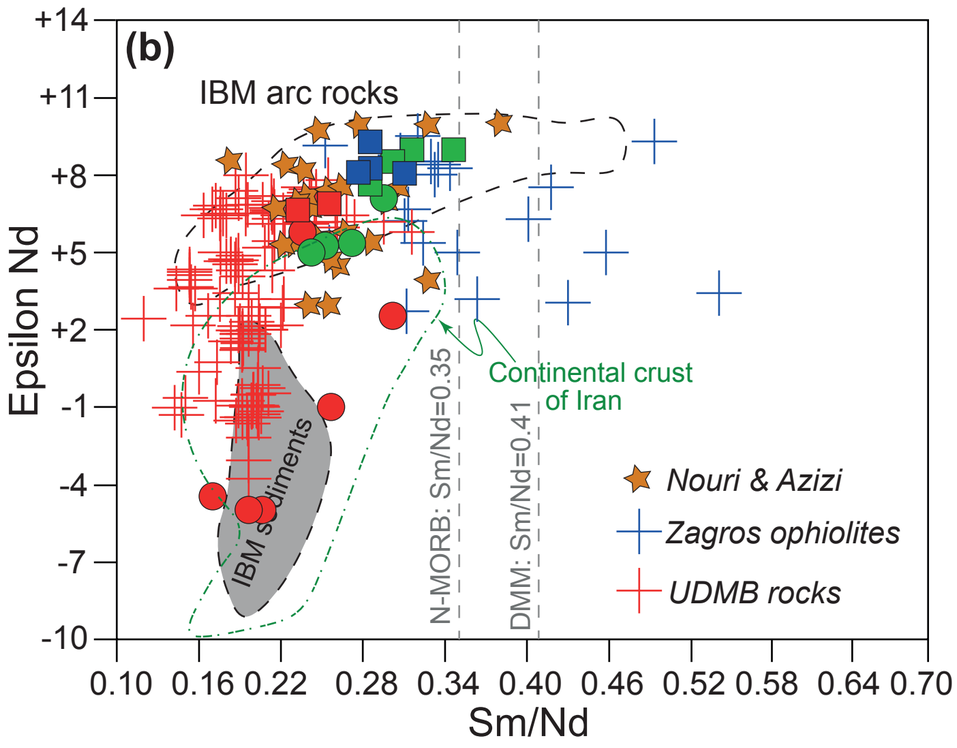

ACCEPTED MANUSCRIPT

Downloaded from http://jgs.lyellcollection.org/ at Helmholtz-Zentrum fur Ozeanforschung Kiel on May 28, 2020

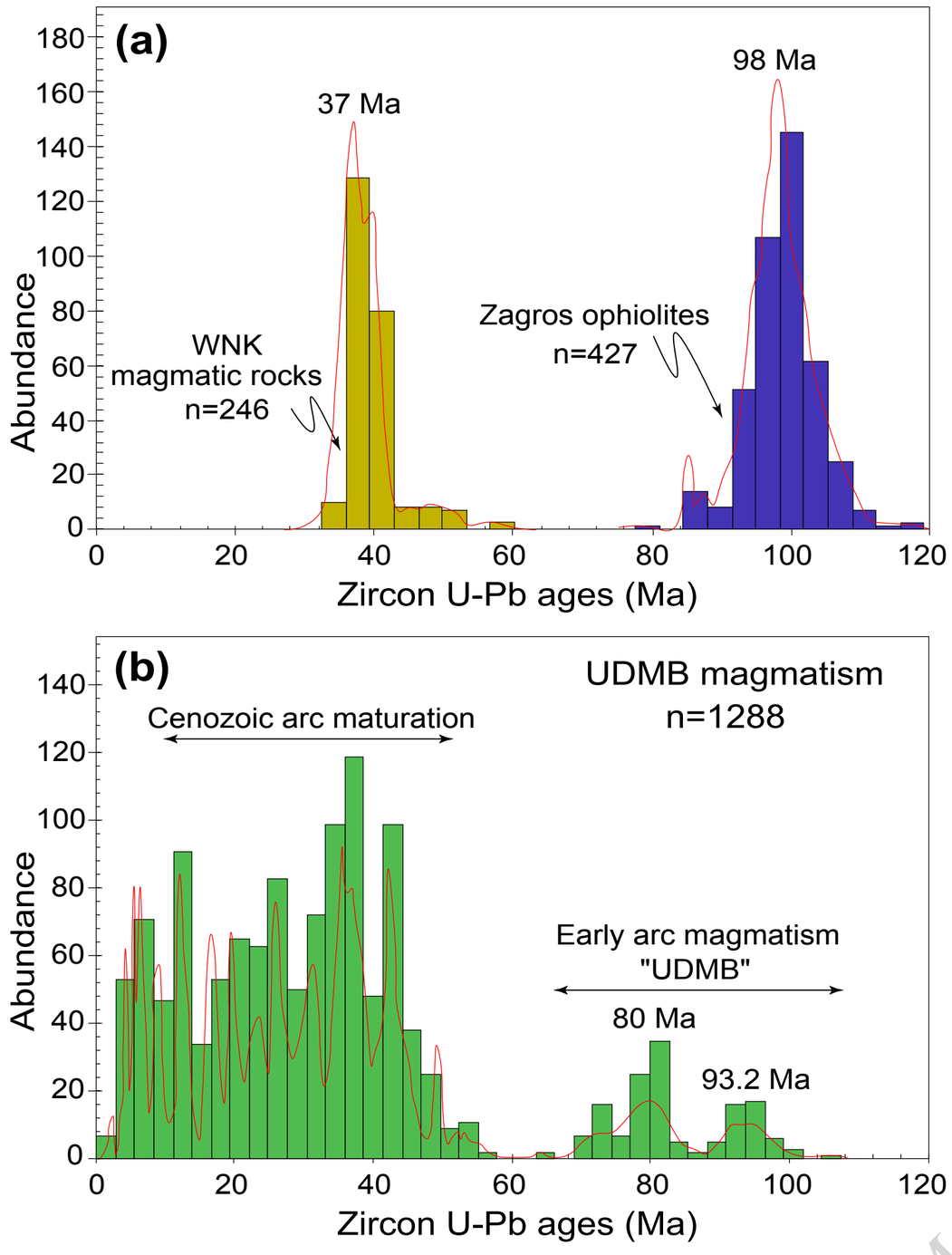

Downloaded from http://jgs.lyellcollection.org/ at Helmholtz-Zentrum fur Ozeanforschung Kiel on May 28, 2020

ACCEPTED MANUSCRIPT

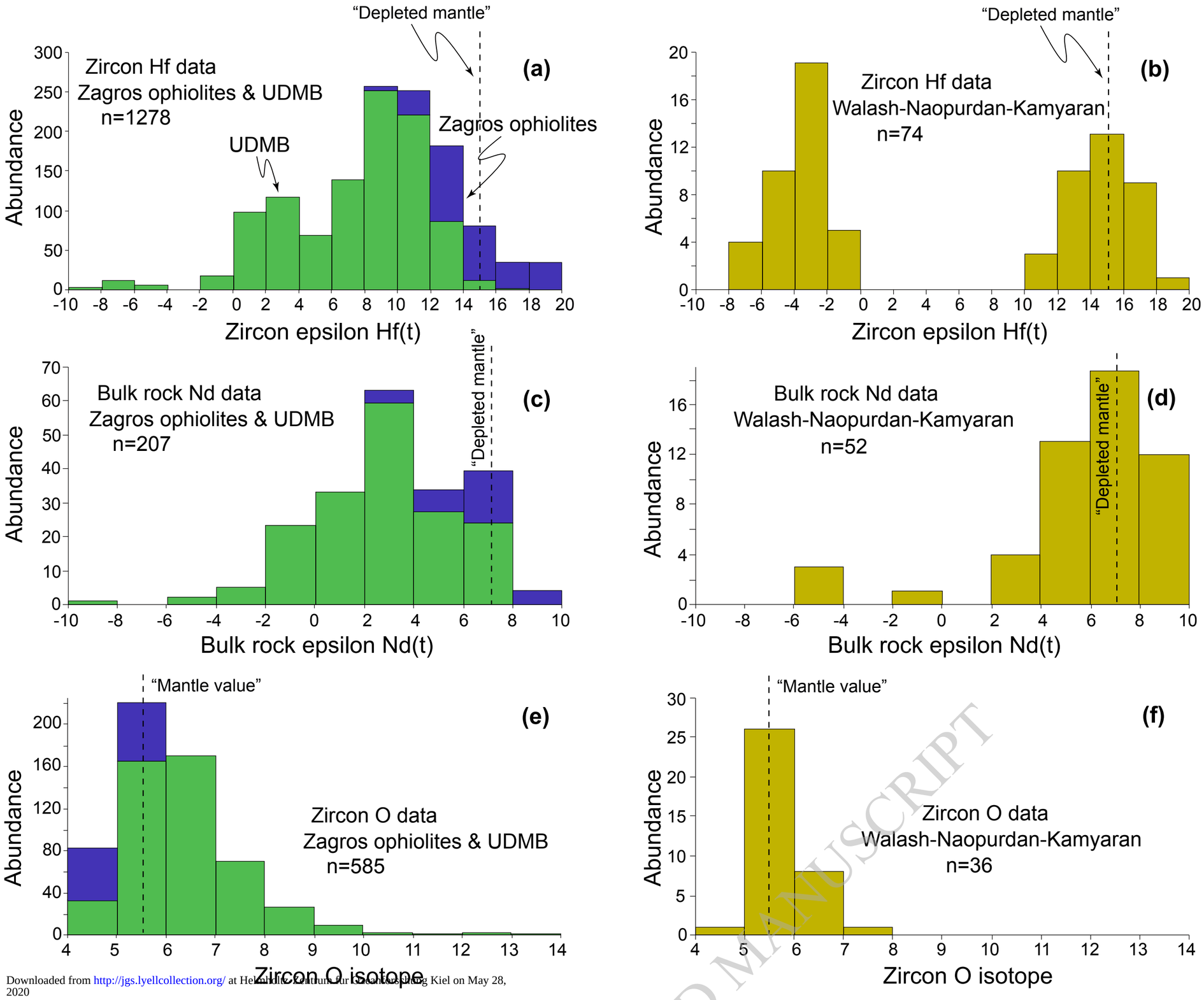

Downloaded from http://jgs.lyellcollection.org/ at Helmholtz-Zentrum für Ozeanforschung Kiel on May 28, 2020

ACCEPTED MANUSCRIPT

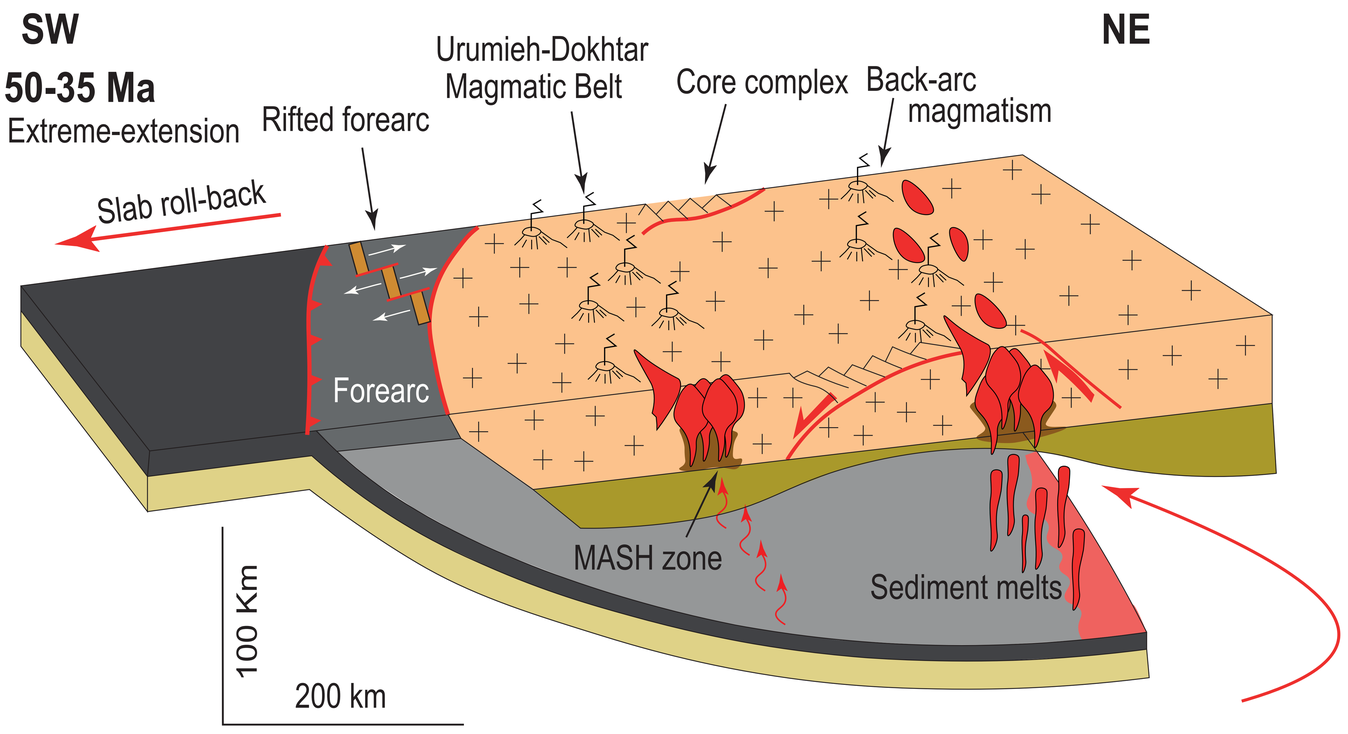

ACCEPTED MANUSCRIPT

Downloaded from http://gs.lyellcollection.org/ at Helmholtz-Zentrum fur Ozeanforschung Kiel on May 28, 2020